



Discover Generics

Cost-Effective CT & MRI Contrast Agents



WATCH VIDEO

AJNR







Fetal MR Imaging Anatomy of the Transverse Temporal Gyrus (Heschl Gyrus)

Eleonora Piccirilli, Chiara Marchetti, Valentina Panara, Claudio Celentano, Francesco D'Antonio, Stefano Sensi, Andrea Righini and Massimo Caulo

This information is current as of June 10, 2025.

AJNR Am J Neuroradiol published online 26 October 2023
<http://www.ajnr.org/content/early/2023/10/26/ajnr.A8026>

Fetal MR Imaging Anatomy of the Transverse Temporal Gyrus (Heschl Gyrus)

 Eleonora Piccirilli,  Chiara Marchetti,  Valentina Panara,  Claudio Celentano, Francesco D'Antonio, Stefano Sensi,  Andrea Righini, and  Massimo Caulo

ABSTRACT

BACKGROUND AND PURPOSE: The human auditory system develops early in fetal life. This retrospective MR imaging study describes the in vivo prenatal anatomic development of the transverse temporal gyrus (Heschl gyrus) site of the primary auditory cortex.

MATERIALS AND METHODS: Two hundred seventy-two MR imaging studies of the fetal brain (19–39 weeks' gestational age) acquired from a single institution's 1.5T scanner were retrospectively examined by 2 neuroradiologists. MR imaging with pathologic findings and extreme motion artifacts was excluded. Postnatal Heschl gyrus landmarks were used as a reference on T2-weighted ssFSE sequences in the 3 orthogonal planes. The frequency of the Heschl gyrus was reported for gestational age, hemisphere, and planes. Descriptive statistics and a McNemar test were performed.

RESULTS: Two hundred thirty MR imaging studies were finally included. Fetal brains were divided by gestational age (in weeks) into 8 groups (parentheses indicate the number of observations): 19–21 (29), 22–23 (32), 24–25 (21), 26–27 (18), 28–29 (35), 30–31 (30), 32–33 (33) and >34 (32). The Heschl gyrus appeared on MR imaging between 24 and 25 weeks' gestational age (14/21 fetuses, 67%) and was visible in all fetuses after the 28th week of gestation. By its appearance (24–28 weeks' gestational age), the sagittal plane was the most sensitive in its detectability. After 28–29 weeks' gestational age, the Heschl gyrus was evident in all acquisition planes and fetuses. Results did not differ between hemispheres.

CONCLUSIONS: The Heschl gyrus appears on MR imaging at 24–25 weeks' gestational age, paralleling the functional activation of the auditory system. We propose the Heschl gyrus as an early additional MR imaging marker of fetal brain development.

ABBREVIATIONS: GA = gestational age; HG = Heschl gyrus; SI = sulcus intermedius; ssFSE = single-shot fast spin-echo

The human auditory system is a unimodal sensory system developed to receive, interpret, and respond to complex language and plays a major role in musical skills.¹ As the acoustic waves reach the auditory receptor cells in the organ of Corti,

sound vibrations are transformed into electric signals. Then, the acoustic nerve transmits the auditory stimuli to the cochlear nuclei in the brainstem, and signals ascend through the auditory pathway to the auditory cortex.

The primary auditory cortex is located in the transverse temporal gyrus and was first described in 1878 by Heschl on post-mortem specimens, and since then, it has been identified as the Heschl gyrus (HG).^{2–4} From an evolutionary perspective, the HG is relatively new because it can be found only in a subset of chimpanzee brains, while it is not present in the macaque monkey.^{5,6}

The HG runs diagonally across the superior temporal plane, hidden in the depth of the Sylvian fissure.⁴ Its characteristic shape and location can be readily identified on MR images using specific landmarks.⁴ Axial images passing through the interthalamic adhesion identify the HG as a thin gyrus running anterior-laterally from the posterior aspect of the insula to the lateral convexity. Coronal and sagittal images passing through the planum temporale identify the HG as having a mushroom- or omega-like shape, respectively.⁷ In adults, the inconstant presence of the sulcus

Received June 11, 2023; accepted after revision August 30.

From the Department of Neuroscience (E.P., S.S., M.C.), Imaging and Clinical Sciences, and Center for Fetal Care and High-Risk Pregnancy (F.D.), Department of Obstetrics and Gynecology, University of Chieti, Chieti, Italy; Neuro-Oncology Unit (E.P.), Department of Imaging, Bambino Gesù Children's Hospital, Istituto di Ricovero e Cura a Carattere Scientifico, Rome, Italy; Radiology Unit (C.M.), San Pio Da Pietrelcina Hospital, Vasto, Chieti, Italy; Department of Radiology (V.P., M.C.), Santissima Annunziata Hospital, Chieti, Italy; Obstetrics and Gynaecology Unit (C.C.), Santo Spirito Hospital, Pescara, Italy; and Neuroradiology Unit (A.R.), Pediatric Radiology Department, Vittore Buzzi Children's Hospital, Milan, Italy; ITAB-Institute of Advanced Biomedical Technologies, Department of Neuroscience, Imaging and Clinical Sciences (E.P., C.M., V.P., S.S., M.C.), University G. d'Annunzio of Chieti-Pescara, Chieti, Italy.

Eleonora Piccirilli and Chiara Marchetti share first authorship.

Please address correspondence to Massimo Caulo, MD, PhD, Department of Neuroscience, Imaging and Clinical Sciences, Institute for Advanced Biomedical Technologies, University G. d'Annunzio of Chieti-Pescara, Via Luigi Polacchi 11, 66100 Chieti, Italy; e-mail: massimo.caulo@unich.it

<http://dx.doi.org/10.3174/ajnr.A8026>

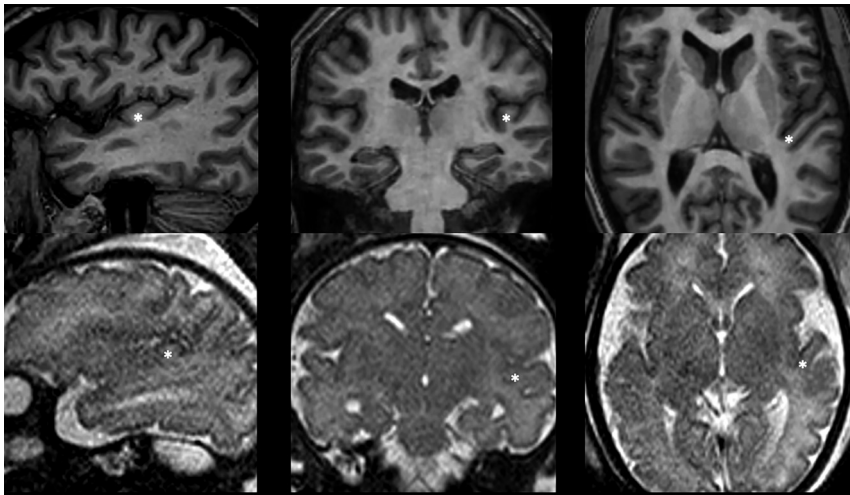


FIG 1. Representative images of adult (*upper row*) and fetal (*lower row*, 28 weeks' GA) HGs on the 3 orthogonal planes. Adult landmarks were used to correctly identify the HG on the fetal brains (*asterisk*).

intermedius (SI) may split the HG, leading to different inter- or intraindividual configurations.⁶ Morphologic variability has been described more often in the right than in the left hemisphere.⁸

Unlike vision, in which the visual experience begins after birth, the auditory system develops in utero and fully functions at birth. Its functional development begins around 25–29 weeks' gestation when the ganglion cells of the spiral nucleus in the cochlea connect the inner cells to the brainstem and the temporal lobe.¹ By 32 weeks' gestational age (GA), fetuses can discriminate tones, mothers' voices, and simple music.⁹ Bilateral activation of the HG by maternal internal acoustic stimulus was demonstrated using blood oxygen level-dependent fMRI between 33 and 38 weeks' GA.⁹ Furthermore, fetuses at 28–32 weeks' GA show a heart rate increase to music stimulation, indicating in utero functioning.¹⁰

Such extensive functional characterization of the auditory cortex in fetuses contrasts with the limited knowledge of its prenatal anatomic development. To date, relatively few studies have concentrated on the prenatal anatomic development of the HG. By sectioning 207 fetal brains in the 3 orthogonal planes, Chi et al¹¹ could recognize the HG from 31 weeks' gestation.

More recently, López Ramón Y Cajal¹² used 3D ultrasound to characterize the in vivo development of the HG in a cohort of 224 human fetuses between 18 and 41 weeks' gestation.

Remarkably, the anatomic development of the HG has never been investigated using prenatal MR imaging, and currently, it is not included among potential markers of normal brain development in clinical fetal MR imaging. Thus, the purpose of the present study was to describe the anatomic development of the transverse temporal gyrus assessed on fetal brain MR imaging.

MATERIALS AND MATERIALS

Study Population

Due to the retrospective nature of the study, the need for ethics committee approval was waived by our institutional review board.

A total of 272 fetal MR images were obtained between June 2019 and August 2022 at the Institute for Advanced Biomedical Technologies of the G. D'Annunzio Chieti-Pescara University. Scans were then retrospectively evaluated.

Fetuses underwent MR imaging for the following indications:

- Suspicion of abnormal CNS and non-CNS features (ventricular dilation, anomalies of cortical development, posterior fossa abnormalities, abnormal fetal brain biometry, extracerebral malformations) as indicated by fetal ultrasound
- Pregnancy at risk: toxoplasmosis, rubella, cytomegalovirus, herpes simplex, and HIV (TORCH) maternal seroconversion, intrauterine growth restriction, twin-to-twin transfusion syndrome
- Family history of genetic disorders.

Scans of fetal brains with physiologic gyration and biometric parameters at MR imaging (according to Parazzini et al¹³ [younger than 24 weeks' GA] and to Garel et al¹⁴ [older than 24 weeks' GA]) were included in the study.¹⁵ Fetal brains with pathologic findings on MR imaging (ie, ventriculomegaly, agenesis of the corpus callosum, posterior fossa malformations, intracerebral hemorrhage, stroke, and malformations of cortical development) were excluded and underwent postnatal MR imaging.

Fetal MR Imaging

Images were acquired on a 1.5T scanner (Achieva; Philips Healthcare) using a 16-channel SENSE XL Torso Coil (Philips Healthcare). Patients were scanned supine. When feasible, the mother was fasting for at least 4 hours to limit fetal motion artifacts.

The standardized fetal brain MR imaging protocol included single-shot fast spin-echo T2-weighted sequences (ssFSE-T2-weighted TSE) in the 3 orthogonal planes (section thickness = 3 mm, in-plane resolution = 1.0–1.2 mm²), axial T1-weighted TSE sequences, and DWI (*b* factors: *b*=0, *b*=500, and *b*=700).

The size of the fetal head determined the FOV.

MR Imaging Analysis

All MR images were analyzed in consensus by 2 neuroradiologists with >5 years' experience in prenatal neuroradiology. Postnatal HG landmarks were used as a reference on T2WI (Fig 1). On axial sections, the HG was visualized on the slice passing through the interthalamic adhesion as an oblique structure of the planum temporale with a posterior-anterior and medial-lateral dislocation.^{7,16} On sagittal and coronal sections, the HG appears as a protrusion above the posterior part of the superior temporal gyrus (Fig 1).^{4–6}

MR images were analyzed in descending order of GA to increase HG detection in earlier stages of fetal life.

On each plane, the HG was classified as “visible” when identified in at least 1 scan plane and “not visible” when uncertain or not identified.

We also tried to evaluate SI detectability. Because the SI splits the HG, leading to a heart-shaped configuration in the sagittal plane, this characteristic feature was used for identification (Fig 2).

Statistical Analysis

HG frequencies were reported for GAs and hemispheres. A McNemar test was performed to compare HG detection between hemispheres using SPSS Statistics for Mac, Version 25.0 (IBM) ($P < .05$).

RESULTS

Fetal Demographics

Of the initial 272 fetal MR images, 230 were eventually included. Seventeen examinations were excluded due to pathologic findings (ventriculomegaly, callosal agenesis, posterior fossa malformations, cerebral hemorrhages, and abnormalities of cortical development), and 25, due to motion artifacts (Fig 3).

The GA ranged from 19 to 39 weeks (mean, 28 weeks; median, 29 weeks).

The cases were subdivided into eight 2-week GA groups: 19–21 GA (29 fetuses), 22–23 GA (32 fetuses), 24–25 GA (21 fetuses),

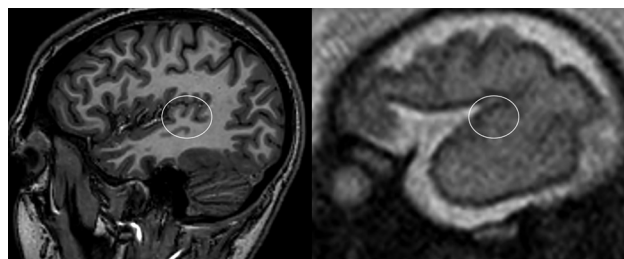


FIG 2. The SI of the HG in representative adult (left) and fetal (right, 28 weeks' GA) brains. The characteristic adult heart-shaped configuration in the sagittal plane was used for SI identification on fetal scans.

26–27 GA (18 fetuses), 28–29 GA (35 fetuses), 30–31 GA (30 fetuses), 32–33 GA (33 fetuses), and >34 GA (32 fetuses). The distribution of fetuses according to GA is given in Figs 3 and 4.

The 2-week GA range was chosen because no substantial changes in gyrational patterns are observed in this timeframe.¹⁵ Fetuses between 34 and 39 weeks' GA were grouped because by the 34th week of GA, all the primary sulci are already present on MR imaging.¹⁵

HG Fetal Development

The HG became visible between 24 and 25 weeks' GA and was detectable in 14/21 fetuses (67% of cases); between 26 and 27 weeks' GA, the HG was detectable in 17/18 fetuses (94% of cases); and by the 28th week of GA onward, the HG was always detectable (Table).

The chart in Figs 4 and 5 summarizes the time of HG appearance in each plane. Figure 6 shows HG changes with GA as assessed on 3 orthogonal planes.

The HG becomes detectable in the earliest gestational weeks of the sagittal plane (24–25 weeks). The structure emerges as a little hump on the posterior part of the superior temporal gyrus. It then reaches a mushroom-like shape abutting the Sylvian fissure from 28 to 29 weeks' GA and further beyond.

On the coronal sections, the HG begins to be visible from 26 to 27 weeks' GA in the upper and most medial part of the superior temporal gyrus. In these earliest stages, the HG emerges as a little point. With GA progression, the HG becomes an evident protrusion, and from the 34 weeks' GA onward, it appears as a hill-shaped structure.

On axial sections, the HG begins to be visible around 26 weeks' GA, when it emerges as a blurred oblique gyrus with a posterior-anterior and medial-lateral course, deep in the lateral fissure. The HG becomes more defined in the intermediate stages of gestation (28–29 and 30–31 weeks) and reaches a thin,

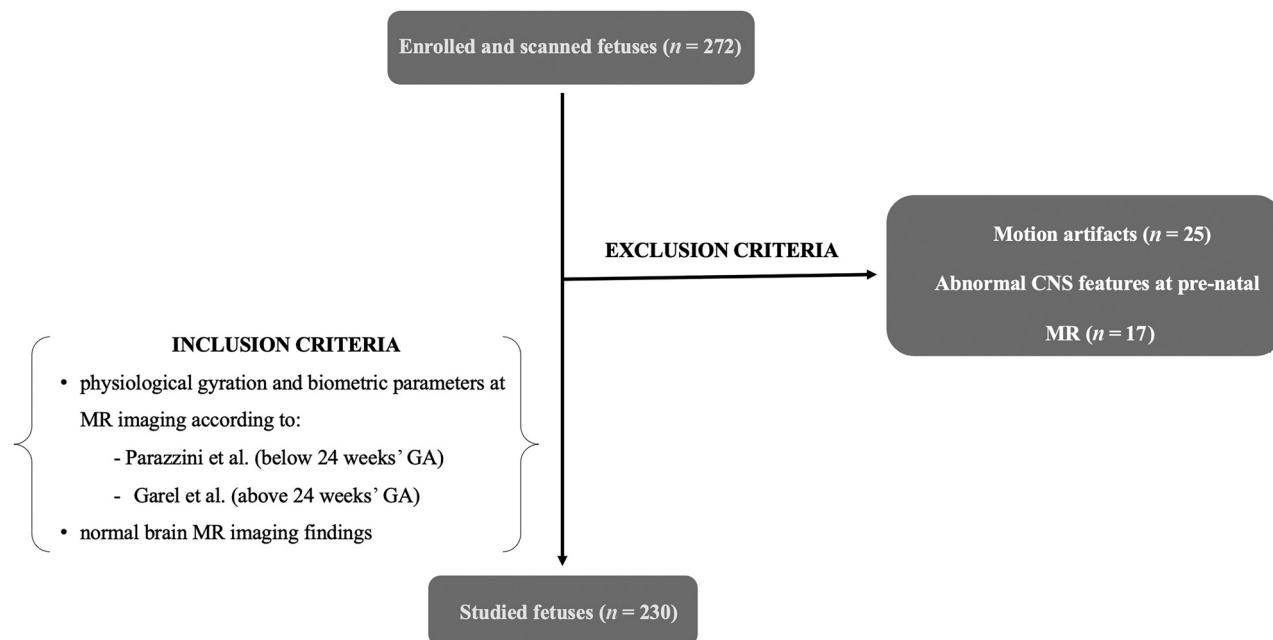


FIG 3. Flow chart detailing inclusion and exclusion criteria.

undulated gyral morphology at the edges of the Sylvian fissure in more advanced GA stages (>32 weeks).

By 28–29 weeks' GA, the HG becomes visible in all fetuses and planes (Table and Figs 5 and 6).

HG and SI

The SI becomes detectable from the 28th to 29th week onward. Of the 103 fetal brains with a GA of >28–29 weeks, the SI was detectable in 30 fetuses (29%).

HG and Hemispheric Differences

No statistically significant differences existed between right and left HG detection ($P = .38$).

DISCUSSION

MR imaging has been used to describe the normal anatomy of the HG in adults and its abnormal development.^{2,8,17} Fetal maturational changes of the HG have been studied using only ultrasound or in ex vivo specimens.^{12,18} Our study focused on the description of HG development as assessed by fetal MR imaging.

We demonstrated that the HG becomes detectable during the second trimester of gestation, specifically between the 24th and 25th week, and that it is visible on MR images in all fetuses from 28 weeks.

Similar to other in vivo sulcations detected by Garel et al,¹⁴ there was a 2-week mean lag time between the first HG detection and its presence in >75% of the cases.

We hypothesized that the early identification of the HG is driven by auditory development during intrauterine life. During

embryogenesis, sulci and gyri develop with a predefined and predictable sequence that reflects their phylogeny and hierarchy so that gyri containing eloquent areas are the first to appear.^{19,20}

Such anatomic development likely underlies a progressive functional maturation. The auditory activity has been demonstrated to begin in utero, because the processing of acoustic stimuli is part of the fetal experience.^{1,21} Graven and Browne¹ found that the human auditory system becomes functional at around 25 weeks' GA, thereby overlapping with the time in which the HG becomes macroscopically detectable. Later, as early as 27 gestational weeks when the HG becomes more defined, MEG studies demonstrated that fetuses can perceive sounds and discriminate them.^{22,23}

At the initial time of its appearance (24–25 weeks' GA), the HG was best demonstrated on the sagittal plane, followed by the coronal plane.

As the HG gets thicker and bulges toward the Sylvian fissure, morphing to its final, adultlike shape, it becomes visible on the axial plane, approximately 4 weeks after its initial detection on the sagittal plane.

The HG tends to develop in an anterior-posterior and oblique and upward fashion, thus explaining the greater sensitivity of the sagittal and coronal planes in its recognition during the earliest stages of gestation.

Likewise, the minimal width of the HG before 28 weeks' GA may account for its limited detectability in the axial plane. It is known that the prenatal recognizability of gyri on imaging usually lags behind their histologic appearance. Our results raise an apparent contradiction between histopathologic and MR imaging data, because the original observations of Chi et al¹⁸ date the appearance of the HG at 31 weeks' GA as assessed on postmortem fetal brain specimens. However, this discrepancy may stem from methodologic issues. In that study,¹⁸ only 20% of the fetal brains were sectioned in the sagittal plane, which we found to be the most sensitive in the earliest phases of HG appearance, possibly owing to its pattern of growth and orientation. Therefore, their relatively late finding¹⁸ likely reflects an underestimation of the actual timing of the appearance of HG. Moreover, brain fixation and consequent tissue shrinking may have impaired the detection of smaller structures, including the HG, in younger fetuses.

Some comments are also required on the study of López Ramón Y Cajal,¹² which, with intrauterine ultrasound, detected the HG well before 24 weeks' gestation. Intrinsic technical differences between ultrasound and prenatal MR imaging, particularly the lower spatial resolution of the latter, should be considered. Therefore, ultrasound data cannot be used as a reference in prenatal MR imaging practice. Both normative data, ours and y Cajal's, need to be confirmed by further studies.

Due to the left hemispheric dominance for language, interhemispheric morphologic differences of the HG have been postnatally investigated in

Frequencies of HG appearance in the three orthogonal planes according to GA groups

GA (week)	Sagittal Plane (%)	Coronal Plane (%)	Axial Plane (%)
19–21	0	0	0
22–23	0	0	0
24–25	67	9.5	0
26–27	94	88.8	67
28–29	100	100	100
30–31	100	100	100
32–33	100	100	100
34–39	100	100	100

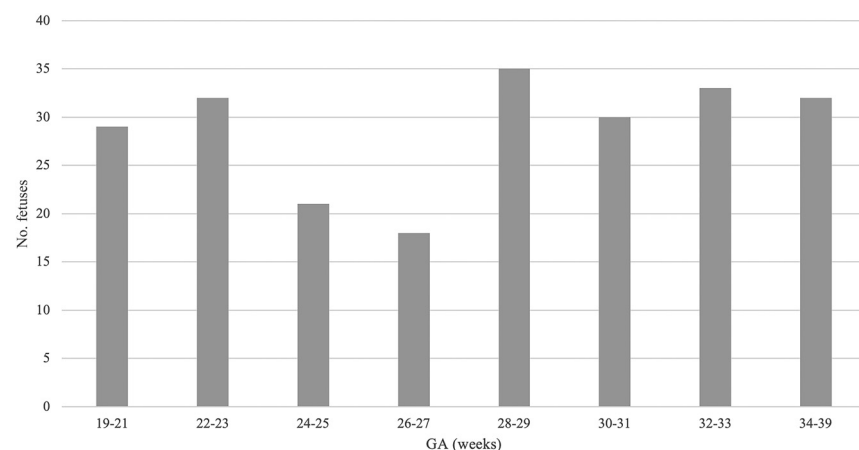


FIG 4. Distribution of the number of fetuses as a function of GA.

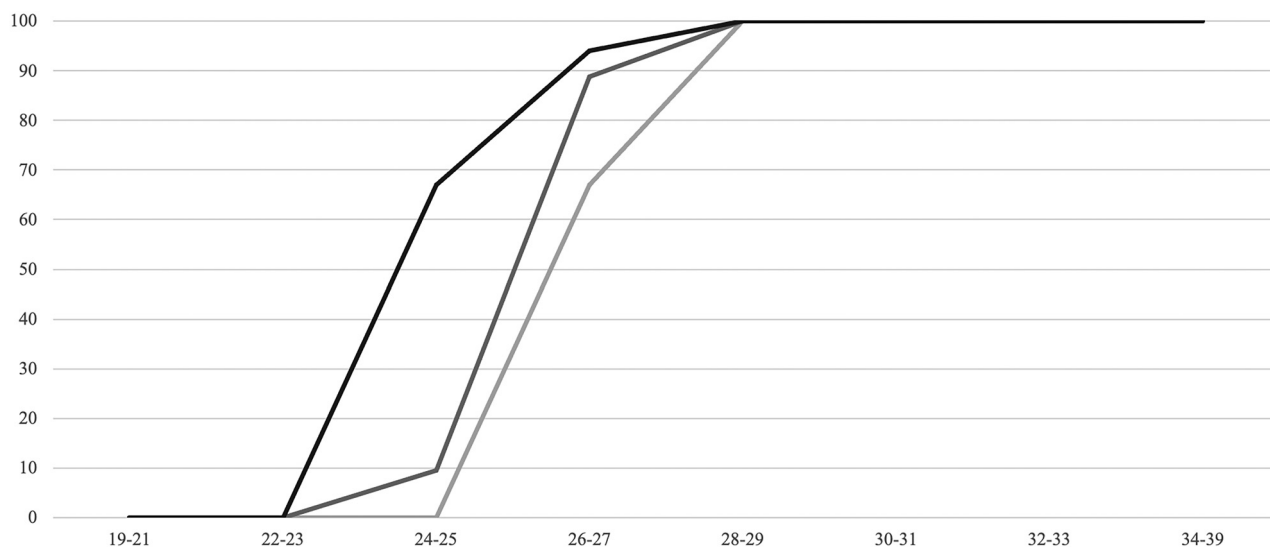


FIG 5. Detection of the HG on sagittal (*black line*), coronal (*gray line*), and axial (*light gray line*) T2-weighted SSh MR images with increasing GA (in weeks).

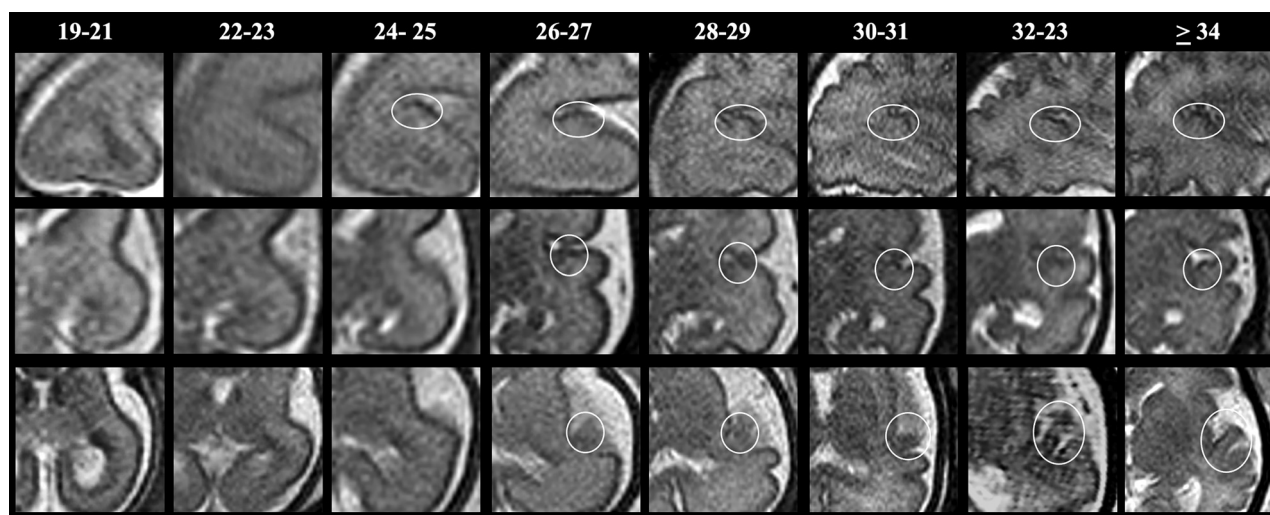


FIG 6. SSh T2WI sagittal (*upper row*), coronal (*middle row*), and axial (*lower row*) MR images illustrating changes in HG morphology with increasing GA.

relation to auditory processing. Furthermore, HG high morphologic variability across individuals and brain hemispheres has been used as a surrogate for functional lateralization.²⁴ Thus, the HG might appear in one hemisphere before the other, though the link between interhemispheric anatomic variability and function remains elusive because the results are inconsistent among studies. Indeed, a rightward asymmetry, a leftward asymmetry, and no asymmetry have all been reported.²⁵⁻²⁷ Such inconsistencies may be biased by the studied features (gyrification versus morphometry/volumetry), handedness, and age, but also by the different examination methods and the complexity of the HG and its sulcal landmarks.^{4,8}

Anatomic investigations of fetuses have revealed that the right HG appears 1-2 weeks earlier than the left and is a more frequent side of duplication.¹¹ On the contrary, although the left HG seemed to slightly anticipate the right in our cohort, we found no significant differences in HG appearance between the 2

hemispheres. Similarly, López Ramón Y Cajal¹² did not observe between-hemisphere differences. Our findings do not necessarily contradict those in previous studies. In that respect, although Chi et al¹¹ reported slight anticipation of the right HG development, statistical significance was not sought. Moreover, the most frequent finding in both MR imaging and postmortem studies is a symmetric single HG in adults,^{2,4,8} thus questioning whether interhemispheric anatomic differences can be considered a reliable marker of functional lateralization.

To add to the complexity of the matter, our findings seem to question whether fetuses exhibit anatomic asymmetry in this area. This feature could emerge later in life as an advantage in sound processing or due to multiple influences. Of note, given the resolution constraints of the sequences used, we did not search for the possibility of hemispheric differences in size and morphology of the HG. In this regard, high-resolution volumetric sequences, such as a 3D-T2 sampling perfection with application-

optimized contrasts by using different flip angle evolution (SPACE sequence; Siemens) or volume isotropic turbo spin-echo acquisition (VISTA), together with the use of stronger magnetic fields allowing higher image quality, would help.

In adults, the HG is variably divided by the presence and the depth of the SI into 4 anatomic variants, single HG, common stem duplication, complete posterior duplication, and multiple duplications that protrude over the posterior part of the superior temporal gyrus in the coronal and sagittal slices as a single omega, a mushroom, a heart, a bow tie, or 2 separate S.⁴ Due to the higher consistency, we used this peculiar heart-shaped configuration of the HG in the sagittal plane as a marker of its presence.

We found that the SI can be detected from 28 to 29 weeks' GA, with a prevalence of 29%. Our results are similar to the reported frequency, ranging between 24% and 33%, in prenatal and postnatal subjects.^{4,12}

However, the SI is a very thin structure. Thus, the resolution threshold of our sequences combined with motion artifacts may have contributed to underestimating its prevalence. The section-thickness constraints have also prevented us from reaching greater anatomic detail.

HG duplication is considered a physiologic, anatomic variant, usually associated with phonologic and musical expertise.²⁸ Nonetheless, HG duplication has been proved to be an important clinical finding. Its increased presence has been reported in patients with learning disabilities, autism, and neuropsychiatric disorders.²⁹⁻³¹ The link between the presence of SI in fetal brains and its clinical and functional significance warrants further investigation.

The study has limitations, including its retrospective design. Also, another difficulty we encountered was the limited spatial resolution of 2D sequences since high-resolution 3D T2 images became part of our routine protocol from January 2023. High-resolution 3D-T2 sequences are of great value in fetal brain biometry to obtain proper orthogonal planes. We also recognize that smaller anatomic structures such as the SI might have been underestimated. However, previous studies on fetal gyration mainly relied on 2D images, which represent the current spatial resolution of prenatal MR imaging to assess primary and secondary sulcation processes. Finally, while beyond the scope of our article, a certain limitation of this study is that clinical correlations between the appearance timeline of the HG and disorders were not explored.

CONCLUSIONS

The HG can be detected on fetal brain MR imaging from 24 to 25 weeks' GA onward, conceivably around the time the auditory system becomes functional. Our normative data about the timing of HG detection could represent an additional marker to be applied to clinical fetal MR imaging.

Disclosure forms provided by the authors are available with the full text and PDF of this article at www.ajnr.org.

REFERENCES

1. Graven SN, Browne JV. **Auditory development in the fetus and infant.** *Newborn Infant Nurs Rev* 2008;8:187-93 [CrossRef](#)
2. Penhune V, Zatorre R, MacDonald J, et al. **Interhemispheric anatomical differences in human primary auditory cortex: probabilistic mapping and volume measurement from magnetic resonance scans.** *Cereb Cortex* 1996;6:661-72 [CrossRef Medline](#)
3. Khalighinejad B, Patel P, Herrero JL, et al. **Functional characterization of human Heschl's gyrus in response to natural speech.** *Neuroimage* 2021;235:118003 [CrossRef Medline](#)
4. Abdul-Kareem IA, Sluming V. **Heschl gyrus and its included primary auditory cortex: structural MRI studies in healthy and diseased subjects.** *J Magn Reson Imaging* 2008;28:287-99 [CrossRef Medline](#)
5. Moerel M, De Martino F, Formisano E. **An anatomical and functional topography of human auditory cortical areas.** *Front Neurosci* 2014;8:225 [CrossRef Medline](#)
6. Benner J, Wengenroth M, Reinhardt J, et al. **Prevalence and function of Heschl's gyrus morphotypes in musicians.** *Brain Struct Funct* 2017;222:3587-603 [CrossRef Medline](#)
7. Yousry TA, Fesl G, Büttner A, et al. **Heschl's gyrus: anatomic description and methods of identification in MRI.** *Int J Neuroradiol* 1997;3:2-12
8. Marie D, Jobard G, Crivello F, et al. **Descriptive anatomy of Heschl's gyri in 430 healthy volunteers, including 198 left-handers.** *Brain Struct Funct* 2015;220:729-43 [CrossRef Medline](#)
9. Goldberg E, McKenzie CA, de Vrijer B, et al. **Fetal response to a maternal internal auditory stimulus.** *J Magn Reson Imaging* 2020;52:139-45 [CrossRef Medline](#)
10. Kisilevsky BS, Hains S, Jacquet AY, et al. **Maturation of fetal responses to music.** *Dev Sci* 2004;7:550-59 [CrossRef Medline](#)
11. Chi JG, Dooling EC, Gilles FH. **Left-right asymmetries of the temporal speech areas of the human fetus.** *Arch Neurol* 1977;34:346-48 [CrossRef Medline](#)
12. López Ramón Y Cajal C. **Antenatal study of the Heschl's gyrus: the first step to understanding learning.** *Med Hypotheses* 2019;130:109290 [CrossRef Medline](#)
13. Parazzini C, Righini A, Rustico M, et al. **Magnetic resonance imaging: brain normal linear biometric values below 24 gestational weeks.** *Neuroradiology* 2008;50:877-83 [CrossRef Medline](#)
14. Garel C, Chantrel E, Elmaleh M, et al. **Fetal MRI: normal gestational landmarks for cerebral biometry, gyration and myelination.** *Childs Nerv Syst* 2003;19:422-25 [CrossRef Medline](#)
15. Garel C, Chantrel E, Brisse H, et al. **Fetal cerebral cortex: normal gestational landmarks identified using MR imaging.** *AJNR Am J Neuroradiol* 2001;22:184-89 [Medline](#)
16. Simon E, Perrot X, Linne M, et al. **Morphometry and localization of the temporal transverse Heschl's gyrus in magnetic resonance imaging: a guide for cortical stimulation of chronic tinnitus.** *Surg Radiol Anat* 2013;35:115-24 [CrossRef Medline](#)
17. Leonard CM, Puranik C, Kuldau JM, et al. **Normal variation in the frequency and location of human auditory cortex landmarks. Heschl's gyrus: where is it?** *Cereb Cortex* 1998;8:397-406 [CrossRef Medline](#)
18. Chi JG, Dooling EC, Gilles FH. **Gyrus development of the human brain.** *Ann Neurol* 1977;1:86-93 [CrossRef Medline](#)
19. Das S, Bal K, Bhattacharjee S. **Morphological development of sulci in fetal brain: an anatomical study.** *Asian J Med Sci* 2022;13:45-50 [CrossRef](#)
20. Nishikuni K, Ribas GC. **Study of fetal and postnatal morphological development of the brain sulci.** *J Neurosurg Pediatr* 2013;11:1-11 [CrossRef Medline](#)
21. Ghio M, Cara C, Tettamanti M. **The brain readiness for speech processing: a review on foetal development of auditory and primordial language networks.** *Neurosci Biobehav Rev* 2021;128:709-19 [CrossRef Medline](#)
22. Schleussner E, Schneider U. **Developmental changes of auditory-evoked fields in fetuses.** *Exp Neurol* 2004;190(Suppl 1):S59-64 [CrossRef Medline](#)
23. Draganova R, Eswaran H, Murphy P, et al. **Serial magnetoencephalographic study of fetal and newborn auditory discriminative evoked responses.** *Early Hum Dev* 2007;83:199-207 [CrossRef Medline](#)

24. Dorsaint-Pierre R, Penhune VB, Watkins KE, et al. **Asymmetries of the planum temporale and Heschl's gyrus: relationship to language lateralization.** *Brain* 2006;129:1164–76 [CrossRef Medline](#)
25. Galaburda A, Sanides F. **Cytoarchitectonic organization of the human auditory cortex.** *J Comp Neurol* 1980;190:597–610 [CrossRef Medline](#)
26. Economo C, Horn L. **Gyral relief, size, and cortical architectonics of the supratemporal surface: their individual and lateral differences.** *Z Ges Neurol Psychiatr* 1930;130:678–757
27. Campain R, Minckler J. **A note on the gross configurations of the human auditory cortex.** *Brain Lang* 1976;3:318–23 [CrossRef Medline](#)
28. Turker S, Reiterer SM, Seither-Preisler A, et al. **“When music speaks”: auditory cortex morphology as a neuroanatomical marker of language aptitude and musicality.** *Front Psychol* 2017;8:2096 [CrossRef Medline](#)
29. Leonard CM, Eckert MA, Lombardino LJ, et al. **Anatomical risk factors for phonological dyslexia.** *Cereb Cortex* 2001;11:148–57 [CrossRef Medline](#)
30. Prigge MD, Bigler ED, Fletcher PT, et al. **Longitudinal Heschl's gyrus growth during childhood and adolescence in typical development and autism.** *Autism Res* 2013;6:78–90 [CrossRef Medline](#)
31. Takahashi T, Sasabayashi D, Takayanagi Y, et al. **Heschl's gyrus duplication pattern in individuals at risk of developing psychosis and patients with schizophrenia.** *Front Behav Neurosci* 2021;15:647069 [CrossRef Medline](#)